
MIND: IMPROVING MULTIMODAL SENTIMENT ANALYSIS VIA MULTIMODAL INFORMATION DISENTANGLEMENT

Weichen Dai*
USTC

Xingyu Li*
Lin Gang Lab

Zeyu Wang
USTC

Pengbo Hu
USTC

Ji Qi
China Mobile Limited

Jianlin Peng
China Mobile Limited

Yi Zhou
USTC

ABSTRACT

Learning effective joint representations has been a central task in multi-modal sentiment analysis. Previous works addressing this task focus on exploring sophisticated fusion techniques to enhance performance. However, the inherent heterogeneity of distinct modalities remains a core problem that brings challenges in fusing and coordinating the multi-modal signals at both the representational level and the informational level, impeding the full exploitation of multi-modal information. To address this problem, we propose the Multi-modal Information Disentanglement (MInD) method, which decomposes the multi-modal inputs into modality-invariant and modality-specific components through a shared encoder and multiple private encoders. Furthermore, by explicitly training generated noise in an adversarial manner, MInD is able to isolate uninformative information, thus improving the learned representations. Therefore, the proposed disentangled decomposition allows for a fusion process that is simpler than alternative methods and results in improved performance. Experimental evaluations conducted on representative benchmark datasets demonstrate MInD’s effectiveness in both multi-modal emotion recognition and multi-modal humor detection tasks. Code will be released upon acceptance of the paper.

1 INTRODUCTION

Recently, there has been a growing interest in Multi-modal Sentiment Analysis (MSA). The comprehension of sentiment is often enhanced by cross-modal input, such as visual, audio, and textual information. Consequently, researchers have focused on developing effective joint representations that integrate all relevant information from the collected data [1], while most of the models rely on designing sophisticated fusion techniques [2] for the exploration of the intra-modal and inter-modal dynamics. Although multi-modal learning has been theoretically shown to outperform uni-modal learning [3], in practice, the modality gap resulting from the inherent heterogeneity of distinct modalities hampers the full exploitation of the inter-modal information for effective multi-modal representations. This phenomenon persists across a broad range of multi-modal models, covering texts, natural images, videos, medical images, and amino-acid sequences [4]. Therefore, prior approaches that address the representations of each modality through a comprehensive learning framework may lead to insufficiently refined and potentially redundant multi-modal representations.

Recent studies have initiated an exploration into the learning of distinct multi-modal representations. Pham et al. [5] translates a source modality to a target modality for joint representations using cyclic reconstruction. Mai et al. [6] also provides a adversarial encoder-decoder classifier framework to learn a modality-invariant embedding space through translating the distributions. But these methods do not explicitly learn the modality-specific representations which reveal the unique characteristic of emotions from different perspectives. By adopting the shared-private learning frameworks [7], Hazarika et al. [8] and Yang et al. [9] attempt to incorporate a diverse set of information by learning different factorized subspace for each modality in order to obtain better representations for fusion. However, their approaches either utilizes simple constraints that fail to guarantee a perfect factorization, or relies on a complex fusion module which may indicate that the extracted information may be unrefined. Moreover, they both neglect the control in the information flow, which could result in the loss of practical information.

Motivated by the above observations, we propose the Multi-modal Information Disentanglement (MInD) approach to deal with the insufficient exploitation of information from heterogeneous modalities. The main strategy is to decompose features of each modality with information optimization. Specifically, the first component is the modality-invariant component, which can effectively capture the underlying commonalities and explore the shared information across modalities. Secondly, we train the modality-specific component to capture the distinctive information and characteristic features. Furthermore, as unknown noise of each modality may be categorized as complementary components, we explicitly train the generated noise in an adversarial manner to enhance the refinement of the learned information and mitigate the impact of un informativeness on the quality of the representations. The combination of the modality-invariant components and the modality-specific components thus enables a more straightforward fusion process compared to alternative methods, resulting in enhanced performance.

The contributions of this paper can be summarized as:

- We propose MInD, a disentanglement-based multi-modal sentiment analysis method driven by information optimization. MInD overcomes the challenge caused by modality heterogeneity via learning modality-invariant and modality-specific representations, thus aiding the subsequent fusion for prediction tasks.
- We explicitly train the generated noise in a novel way to improve the quality of learned representations. To the best of our knowledge, we are the first work to model un informativeness for a better shared-private disentanglement in MSA.
- MInD outperforms previous state-of-the-art methods on several standard multi-modal benchmarks only with a simple fusion strategy, which demonstrates the power of MInD in capturing diverse facets of multi-modal information.

2 RELATED WORKS

2.1 Multi-modal Sentiment Analysis

Learning effective joint representations is a critical challenge in MSA. Many previous works have contributed to sophisticated fusion techniques. Zadeh et al. [2] proposed tensor-based fusion network which applies outer product to model the uni-modal, bimodal and tri-modal interactions. Mai et al. [6] introduced graph fusion network which regards each interaction as a vertex and the corresponding similarities as weights of edges. Besides, the attention mechanisms [10] are widely used to identify important information [11, 12, 13]. For instance, Tsai et al. [14] developed a novel transformer architecture that effectively integrates unaligned data from different modalities by directional pairwise cross-modal attention. Shenoy et al. [11] assigned weights to the importance differences between multiple modalities through the importance attention network. Delbrouck et al. [15] utilized a Transformer-based joint-encoding (TBJE) model, incorporating modular co-attention and a glimpse layer to effectively encode and analyze emotions and sentiments from one or more modalities. However, as multi-modal inputs have various characteristics and information properties, this inherent heterogeneity of different modalities complicates the analysis of data, thus leading to a significant challenge on the mining and integration of information and the learning of multi-modal joint embedding.

2.2 Disentanglement Learning

Disentanglement learning [7, 16] is designed to unravel complex data structures, isolating key components to extract desirable information for more insightful and efficient data processing. Therefore, this approach plays a pivotal role in aligning semantically related concepts across different modalities and effectively alleviates the problems caused by the modality gap. Furthermore, disentanglement learning significantly contributes to multi-modal fusion by offering a more structured and explicit representation [8]. Such clarity and organization in the data representation are instrumental in enhancing the efficacy and precision of multi-modal integration processes. For this reason, following Salzmann et al. [17], many works have extended the shared-private learning strategies in various scenarios for excellent results, including retrieval [18], user representation in social network [19], and emotion recognition [9], etc. In comparison, to the best of our knowledge, we provide the first attempt that explicitly train the generated noise in addition to the modality-invariant and modality-specific components for a better disentangled decomposition in MSA.

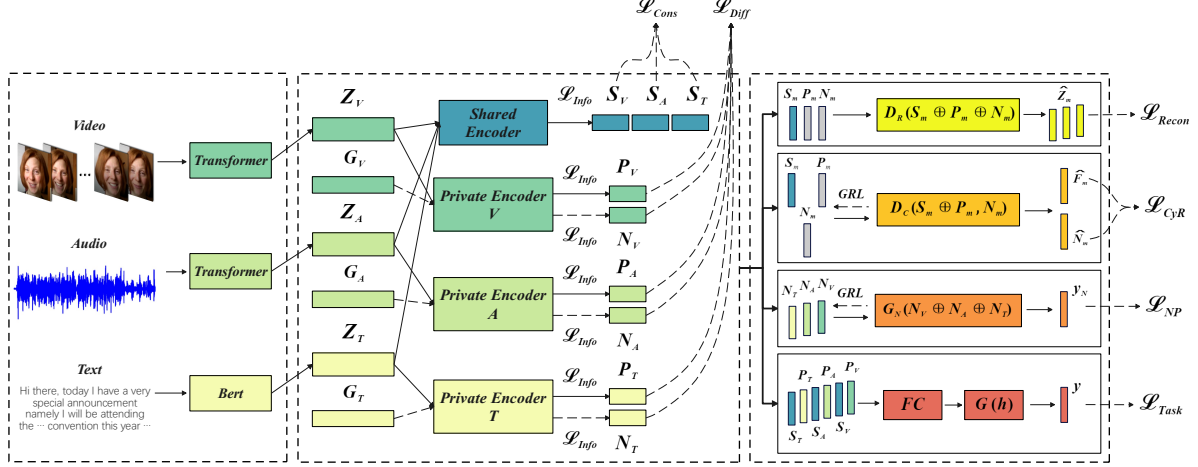


Figure 1: Our proposed model. Each embedding Z_m from the backbones is fed into a shared encoder and multiple private encoders to generate modality-invariant components S_m and modality-specific components P_m , respectively. Meanwhile, by passing Gaussian noise G_m to the private encoders, we align the uninformativeness within the feature subspace. This process is guided by mutual information maximization, the consistency loss and difference loss. After that, we proposed the vanilla reconstruction module, the cyclic reconstruction module and the noise prediction module to further improve the representations.

3 METHOD

3.1 Model Overview

The overall framework of MInD is shown in Fig.1. We introduce our method within the context of a task scenario that incorporates three distinct modalities, namely visual, audio, and text. Each individual data point consists of three sequences of low-level features originating from the visual, acoustic, and textual modalities. We denote them as $\mathbf{X}_V \in \mathbf{R}^{L_V \times d_V}$, $\mathbf{X}_A \in \mathbf{R}^{L_A \times d_A}$, $\mathbf{X}_T \in \mathbf{R}^{L_T \times d_T}$, respectively, where $L_{(\cdot)}$ is the sequence length and $d_{(\cdot)}$ is the embedding dimension.

In response to the challenges posed by modality heterogeneity, we aim to identify an approach that effectively mitigates the distributional discrepancy and enhances the information extraction, ensuring a comprehensive analysis of multi-modal inputs. To this end, we decompose the inputs into two parts: the modality-invariant components and the modality-specific components. The uninformativeness is modeled starting from generated Gaussian noise which is sent to the corresponding private encoder for feature subspace alignment, see details and explanation in the following subsections. These representations are then facilitated through the implementation of information constraints, consistency constraints, and difference constraints. The integration of these constraints contributes to better utilization of information embedded within the high-level feature, enabling efficient exploration of both cross-modal commonality and distinctive features. After that, we evaluate the completeness of decomposed information through a vanilla reconstruction module. Moreover, we employ a cyclic reconstruction module to further reduce information redundancy, and a noise prediction module to minimize the task-related information within the trained noise. The modality-invariant components and the modality-specific components are finally fused for prediction tasks.

3.2 Feature Extraction

Here we employ transformer-based models [10] to extract high-level semantic features from individual modalities. Specifically, we use the Bert [20] model for text modality, and we employ a standard transformer model for the remaining two modalities,

$$Z_m = F^m(X_m; \theta_m), \quad m \in \{V, A, T\}. \quad (1)$$

The refined features of each modality are in a fixed dimension as $Z_m \in \mathbf{R}^{d_k}$.

3.2.1 Modality-Invariant and -Specific Components.

While temporal model-based feature extractors effectively capture the long-range contextual dependencies presented in multi-modal sequences, they fail to effectively handle feature redundancy due to the divergence of different

modalities [21]. Furthermore, the efficacy of the divide-and-conquer processing pattern is affected by the inherent heterogeneity among different modalities.

Inspired by these observations, we employ the shared and private encoders to learn the modality-invariant components and the modality-specific components, which are designed to capture commonality and specificity of individual modalities, respectively. We denote the shared encoder as $E_S(\cdot; \theta_S)$, and the private encoders as $E_{P_m}(\cdot; \theta_{P_m})$, where $m \in \{V, A, T\}$. Then the representations are formulated as below:

$$S_m = E_S(Z_m; \theta_S), \quad (2)$$

$$P_m = E_{P_m}(Z_m; \theta_{P_m}), \quad (3)$$

with $S_m, P_m \in \mathbf{R}^{d_k}$. The shared encoder $E_S(\cdot; \theta_S)$ shares the parameters θ_S across all modalities, while the private encoders $E_{P_m}(\cdot; \theta_{P_m})$ assign separate parameters θ_{P_m} for each modality. Both the shared encoder and private encoders are implemented as simple linear network with the activation function of GeLU [22].

3.2.2 Modeling Uninformativeness.

While the integration of modality-invariant and modality-specific components facilitates a comprehensive representation of multi-modal inputs in former works [8, 9], we argue that this kind of approaches has not yet reached its full potential. The main problem lies in the persistence of meaningless information within the desired representations, for example, modality-specific unknown noise may be categorized as complementary components. This may compromise information purity and limit the model’s expressive capacity. It is infeasible to directly isolate the noise from the modality-specific components as there lacks ground-truth nor any reference signal. Instead, drawing inspiration from adversarial training, we adopted an indirect approach for such separation. Our novel idea is that the private encoders should distinguish the informative input signals from the uninformativeness, mapping them into distinct areas. To this end, we first generate Gaussian noise vectors which are subsequently aligned into feature subspace using the same private encoders, namely:

$$G_m \sim \mathcal{N}(0, 1), \quad N_m = E_{P_m}(G_m; \theta_{P_m}), \quad (4)$$

where $m \in \{V, A, T\}$. We further require the outputs of a private encoder for the normal input Z_m and the noise to be different through constraints, as described in next subsection. This strengthens the robustness of the learned representations and aids in the extraction of more refined, purer information.

3.3 Representation Objectives

3.3.1 Information Constraint.

A conventional approach to discover useful representations involves maximizing the mutual information (MI) between the input and output of models. However, MI is notoriously difficult to compute, especially in continuous and high-dimensional contexts. Recent solution [23] leverage mutual information constraint that estimate and maximize the MI between input data and learned high-level representations simultaneously. Specifically, we employ the objective function based on the Jensen-Shannon divergence here, due to its proven stability and alignment with our primary aim of maximizing MI rather than obtaining an precise value. The estimator is shown below:

$$\begin{aligned} \hat{\mathcal{I}}_{\omega, \theta}^{(JSD)}(Z; E_{\theta}(Z)) = & E_{\mathcal{P}(Z, E_{\theta}(Z))}[-sp(-T_{\omega}(Z, E_{\theta}(Z)))] \\ & - E_{\mathcal{P}(Z) \times \mathcal{P}(E_{\theta}(Z))}[sp(T_{\omega}(Z, E_{\theta}(Z)))], \end{aligned} \quad (5)$$

where $E_{\theta}(Z)$ is the encoder parameterized by θ , $\mathcal{P}(\cdot)$ is the empirical probability distribution, $sp(z) = \log(1 + e^z)$ is the softplus function, and $T_{\omega} : \mathcal{X} \times \mathcal{Y} \rightarrow \mathbf{R}$ is a discriminator function modeled by a neural network with parameters ω called the statistics network.

Since the modality-invariant components are expected to capture cross-modal commonality, we calculate the MI between the outputs and the combination of inputs. We also maximize the MI between the noise outputs and the generated Gaussian noise, encouraging N_m to remain as less informative as the noise inputs after alignment through private encoders. We denote the above procedure as following:

$$\begin{aligned} \mathcal{L}_{Info} = & \sum_{m \in \{V, A, T\}} -\hat{\mathcal{I}}_{\omega_S, \theta_S}^{(JSD)}(Z_V \oplus Z_A \oplus Z_T; S_m) \\ & + \sum_{m \in \{V, A, T\}} -\hat{\mathcal{I}}_{\omega_{P_m}, \theta_{P_m}}^{(JSD)}(Z_m; P_m) \\ & + \sum_{m \in \{V, A, T\}} -\hat{\mathcal{I}}_{\omega_{P_m}, \theta_{P_m}}^{(JSD)}(G_m; N_m). \end{aligned} \quad (6)$$

3.3.2 Consistency Constraint.

Inspired by [24], we introduce the Barlow Twins loss (BT loss) to be the consistency constraint. BT loss is originally designed for learning embedding which are invariant to distortions of the input sample, it forces two embedding vectors to be similar by making the cross-correlation matrix as close to the identity matrix as possible, which minimizes the redundancy between the components of these vectors. Concretely, each representation pair S^A, S^B is normalized to be mean-centered along the batch dimension as $S^{A,nor}, S^{B,nor}$, such that each unit has mean output 0 over the batch. The normalized matrices can be then utilized to depict the cross-correlation matrix:

$$C_{ij}^{A,B} = \frac{\sum_b s_{b,i}^{A,nor} s_{b,j}^{B,nor}}{\sqrt{\sum_b (s_{b,i}^{A,nor})^2} \sqrt{\sum_b (s_{b,j}^{B,nor})^2}}, \quad (7)$$

where b indexes batch samples and i, j index the vector dimension of the networks' outputs. The BT loss is expressed as:

$$\mathcal{L}_{BT}^{m_1, m_2} = \sum_i (1 - C_{ii}^{m_1, m_2})^2 + \lambda_{BT} \sum_i \sum_{j \neq i} (C_{ij}^{m_1, m_2})^2. \quad (8)$$

In the purpose of exploring shared information and commonality across modalities, we transfer the concept into our case by treating different modalities as different views. Following the observations in [25], we set λ_{BT} to be the dimension of the embedding, and calculate the BT loss between the modality-invariant components of each modalities pair:

$$\mathcal{L}_{Cons} = \sum_{(m_1, m_2)} \mathcal{L}_{BT}^{m_1, m_2}. \quad (9)$$

3.3.3 Difference Constraint.

Since both the modality-invariant components and the modality-specific components are learned from the same high-level features Z_m , it may result in the redundancy of information. Moreover, as explained in former subsections, private encoders should effectively differentiate between informative and uninformative inputs. For this sake, we employ the Hilbert-Schmidt Independence Criterion (HSIC) [26] to measure independence. Formally, the HSIC constraint between any two representations R_1, R_2 is defined as:

$$HSIC(R_1, R_2) = (n-1)^{-2} \text{Tr}(U K_1 U K_2), \quad (10)$$

where K_1 and K_2 are the Gram matrices with $k_{1,ij} = k_1(r_1^i, r_1^j)$ and $k_{2,ij} = k_2(r_2^i, r_2^j)$. $U = I - (1/n)ee^T$, where I is an identity matrix and e is an all-one column vector. In our setting, we use the inner product kernel function for K_1 and K_2 . To augment the distinction among individual components, the overall difference constraint is expressed as:

$$\mathcal{L}_{Diff} = \sum_{(R_1, R_2)} HSIC(R_1, R_2), \quad (11)$$

where (R_1, R_2) is the pair from (S_m, P_m) , (S_m, N_m) , (P_{m_1}, P_{m_2}) , and (P_m, N_m) .

3.3.4 Reconstruction Constraint.

We adopt a vanilla reconstruction constraint, which aims to help the combination of representations capture more comprehensive information of their respective modality. Note that we include N_m during the reconstruction, as in our assumption that the modality-invariant components and the modality-specific components contain no meaningless information compared to the original signals. By employing a decoder function

$$\hat{Z}_m = D_R(S_m \oplus P_m \oplus N_m), \quad (12)$$

the reconstruction constraint is then designed as the mean squared error between Z_m and \hat{Z}_m :

$$\mathcal{L}_{Recon} = \frac{1}{3} \sum_{m \in \{V, A, T\}} \frac{\|Z_m - \hat{Z}_m\|_2^2}{d_k}, \quad (13)$$

where $\|\cdot\|_2^2$ is the squared L_2 -norm.

We further minimize the MI between the informative and uninformative vectors through cyclic-reconstruction and gradient-reversal layers [27]. Let F_m be the concatenation of S_m and P_m . $D_C(\cdot; \theta_{F_m})$, $D_C(\cdot; \theta_{N_m})$ be the decoders

for reconstruction from F_m to N_m and from N_m to F_m , respectively. The objective is then formulated as below:

$$\begin{aligned}\mathcal{L}_{CyR} = & \sum_{m \in \{V, A, T\}} \|F_m - D_C(GRL(N_m); \theta_{N_m})\|_2^2 \\ & + \sum_{m \in \{V, A, T\}} \|N_m - D_C(GRL(F_m); \theta_{F_m})\|_2^2,\end{aligned}\quad (14)$$

where $GRL(\cdot)$ is a gradient reversal layer.

3.4 Prediction

Until now, the information disentanglement has been conducted in the unsupervised manner. We now complete our final objective function with the downstream task. The learned modality-invariant and modality-specific components are first fused by a simple linear layer with dimension reduction, and subsequently trained via shallow MLPs: $G(\cdot; \theta_G)$ with several hidden layers and GeLU activation to get the prediction denoted as $\{\hat{y}_i\}$ or \hat{Y} :

$$h = FC(S_V \oplus S_A \oplus S_T \oplus P_V \oplus P_A \oplus P_T), \quad (15)$$

$$\hat{Y} = G(h). \quad (16)$$

Thanks to the explicit modeling of noise, the proposed disentangled decomposition allows for a fusion process that is simpler than alternative methods and results in improved performance.

Specifically, to further reduce the task-related information inside the trained noise (thus the trained noise can be more meaningless in the sense of both informatics and task), we devise a noise-prediction loss with another shallow MLPs: $G_N(\cdot; \theta_{G_N})$, for the prediction $\{\hat{y}_{N,i}\}$ or \hat{Y}_N from noise:

$$\hat{Y}_N = G_N(GRL(N_V \oplus N_A \oplus N_T); \theta_{G_N}), \quad (17)$$

$$\mathcal{L}_{NP} = -\frac{1}{n} \sum_{i=1}^n y_i \cdot \log \hat{y}_{N,i} \quad \text{or} \quad \frac{1}{n} \|Y - \hat{Y}_N\|_2^2. \quad (18)$$

The final objective function is computed as:

$$\begin{aligned}\mathcal{L}_{all} = & \mathcal{L}_{Task} + \mathcal{L}_{NP} + \alpha \mathcal{L}_{Info} \\ & + \beta \mathcal{L}_{Cons} + \gamma \mathcal{L}_{Diff} + \lambda (\mathcal{L}_{Recon} + \mathcal{L}_{CyR}).\end{aligned}\quad (19)$$

The seven loss terms are necessary and serve for different purposes, yet the final loss is controlled by only four hyper-parameters. Here, $\alpha, \beta, \gamma, \lambda$ determine the contribution of each corresponding constraint to the overall loss. And \mathcal{L}_{Task} is the prediction loss, where we employ the standard cross-entropy loss for the classification task, and the mean error loss for the regression task.

4 EXPERIMENTS

4.1 Datasets and evaluation criteria

In this paper, we choose three multi-modal dataset for evaluation, namely CMU-MOSI and CMU-MOSEI for emotion recognition, and UR-FUNNY for humor detection.

4.1.1 CMU-MOSI.

CMU-MOSI [28] is a widely-utilized dataset for MSA. The dataset is collected from 2199 opinion video clips from YouTube, which is splited to 1284 samples for training set, 229 samples for validation set, and 686 samples for testing set, with sentiment score ranges from -3 to 3 for each sample. Same as previous works, we adopt the 7-class accuracy (Acc-7), the binary accuracy (Acc-2), mean absolute error (MAE), the Pearson Correlation (Corr), and the F1 score for evaluation.

4.1.2 CMU-MOSEI.

CMU-MOSEI [29] is a similar but larger dataset that contains 22,856 movie review video clips from YouTube, including 16,326 training samples, 1,871 validation samples, and 4,659 testing samples. Each sample also has a sentiment scores ranging from -3 to 3. The same metrics are employed as in the above setting.

Models	CMU-MOSI					CMU-MOSEI					UR-FUNNY
	Acc7↑	Acc2↑	F1↑	MAE↓	Corr↑	Acc7↑	Acc2↑	F1↑	MAE↓	Corr↑	Acc2↑
TFN	34.9	80.8	80.7	0.901	0.698	50.2	82.5	82.1	0.593	0.700	68.57
LMF	33.2	82.5	82.4	0.917	0.695	48.0	82.0	82.1	0.623	0.677	67.53
MFM	35.4	81.7	81.6	0.877	0.706	51.3	84.4	84.3	0.568	0.717	-
ICCN	39.0	83.0	83.0	0.862	0.714	51.6	84.2	84.2	0.565	0.713	-
MuT	40.0	83.0	82.8	0.871	0.698	51.8	82.5	82.3	0.580	0.703	-
Self-MM	-	85.9	85.9	0.713	0.798	-	85.1	85.3	0.530	0.765	-
HyCon	46.6	85.2	85.1	0.713	0.790	52.8	85.4	85.6	0.601	0.776	-
BBFN	45.0	84.3	84.3	0.776	0.755	54.8	86.2	86.1	0.529	0.767	71.68
CubeMLP	45.5	85.6	85.5	0.770	0.767	54.9	85.1	84.5	0.529	0.760	-
Liu et al.	-	83.7	84.2	0.769	0.783	-	85.0	85.0	0.573	0.741	-
AOBERT	40.2	85.6	86.4	0.856	0.700	54.5	86.2	85.9	0.515	0.763	70.82
SURGM	-	84.5	84.5	0.723	0.798	-	85.0	85.1	0.541	0.758	-
ConFEDE	42.3	85.5	85.5	0.742	0.784	54.9	85.8	85.8	0.522	0.780	-
AcFormer	44.2	85.4	85.2	0.715	0.794	54.7	86.5	85.8	0.531	0.786	-
TCHF	44.8	86.1	86.3	0.748	0.780	53.2	86.3	86.5	0.538	0.770	-
Self-HCL	-	84.9	85.0	0.711	0.788	-	85.9	85.9	0.531	0.775	-
MISA	42.3	83.4	83.6	0.783	0.761	52.2	85.5	85.3	0.555	0.756	70.61
FDMER	44.1	84.6	84.7	0.724	0.788	54.1	86.1	85.8	0.536	0.773	71.87
MInD(ours)	46.6	86.0	86.0	0.711	0.791	53.9	86.6	86.7	0.529	0.772	72.55

Table 1: Performance compared with the SOTA approaches in CMU-MOSI, CMU-MOSEI and UR-FUNNY, with MInD’s results highlighted in bold. According to the comparison, while some baseline methods may stand out when evaluated by specific metric on one dataset, only MInD exhibits consistently competitive performance across all datasets under all metrics.

4.1.3 URFUNNY.

UR-FUNNY [30] dataset contains 16,514 samples of multi-modal punchlines labeled with a binary label for humor/non-humor instance from TED talks, which is partitioned into 10,598 samples in the training set, 2,626 in the validation set, and 3,290 in the testing set. We report the binary accuracy (Acc-2) for this binary classification task.

4.2 Implementation Details

Following recent works, we utilize the pretrained BERT-base-uncased model to obtain a 768-dimension embedding for textual features. Specifically, since the original transcripts are not available for our considered UR-FUNNY version, we follow the same procedure as [8] to retrieve the raw texts from Glove [31]. The acoustic features are extracted from COVAREP [32], where the dimensions are 74 for MOSI/MOSEI and 81 for UR-FUNNY. Moreover, we use Facet² to extract facial expression features for both MOSI and MOSEI, and OpenFace [33] for UR-FUNNY. The final visual feature dimensions are 47 for MOSI, 35 for MOSEI, and 75 for UR-FUNNY.

Our model is built on the Pytorch 2.0.1 with one single Nvidia 3090 GPU. The number of transformer encoder layers for visual and audio are both 3. For the MOSI, MOSEI and UR-FUNNY benchmarks, the batch sizes and epochs are 32 and 100, respectively.

4.3 Comparison With SOTA Models

4.3.1 Baselines.

We compare our model with many baselines, including pure learning based models such as TFN [2], LMF [34], MFM [35], and MuT [14]. Besides, we also compare our model with feature space manipulation approaches like ICCN [36], MISA [8], Self-MM [37], HyCon [38], BBFN [39], FDMER [9] and CubeMLP [40]. Moreover, the more recent and competitive methods, Liu et al. [41], AOBERT [42], SURGM [43], ConFEDE [44], AcFormer [45], TCHF [46] and Self-HCL [47] are also taken into our consideration. Results are directly taken from their corresponding paper.

²<https://imotions.com/platform/>

Models	CMU-MOSI		CMU-MOSEI		UR-FUNNY
	MAE↓	Corr↑	MAE↓	Corr↑	Acc2↑
MInD	0.711	0.791	0.529	0.772	72.55
Role of Modality					
w/o visual	0.857	0.771	0.541	0.770	71.12
w/o Audio	0.759	0.786	0.547	0.764	70.79
w/o Text	1.452	0.051	0.841	0.209	49.67
Role of Disentanglement					
w/o M-Invariant	0.793	0.778	0.546	0.767	70.30
w/o M-Specific	0.777	0.773	0.550	0.772	70.91
Non-Disentangled	0.925	0.753	0.576	0.772	68.97
Role of Constraint					
w/o \mathcal{L}_{Info}	0.755	0.778	0.542	0.761	71.22
w/o \mathcal{L}_{Cons}	0.789	0.777	0.551	0.760	72.28
w/o \mathcal{L}_{Diff}	0.768	0.769	0.556	0.762	71.70
w/o \mathcal{L}_{Recon}	0.727	0.784	0.558	0.758	72.01
w/o \mathcal{L}_{CyR}	0.787	0.773	0.539	0.763	72.28
w/o \mathcal{L}_{NP}	0.732	0.783	0.532	0.771	72.46
Only \mathcal{L}_{Task}	0.788	0.784	0.546	0.768	71.64

Table 2: Results of ablation studies.

4.3.2 Multi-modal Emotion Recognition.

As shown in Tab.1, MInD outperforms each baseline on most or even all evaluation metrics. While some baseline methods may stand out when evaluated by specific metric on one dataset, only MInD exhibits consistently competitive performance across all datasets under all metrics. Specifically, on the MOSI dataset, our approach shows the best results on Acc-7 and MAE, while on the MOSEI dataset, MInD surpasses all the SOTA Acc-2 and the F1 scores. Although on MOSEI, Acc-7 of our approach is relatively lower than SOTA, it could be attributed to the fact that MInD only adopts simple concatenation and shallow linear network for fusion and prediction, which limits fine-grained sentiment calculation on larger dataset. However, we still achieve overall satisfactory results without sophisticated fusion strategy, which reveals that our approach is able to capture sufficiently distinct information to form a comprehensive view of multi-modal inputs. Notably, MInD significantly improves the performance on both datasets compared to MISA [8] and FDMER [9], which are also disentanglement-based methods. This is attributed to our introduction of trained noise that aids in the extraction of more refined, purer information through adversarial learning.

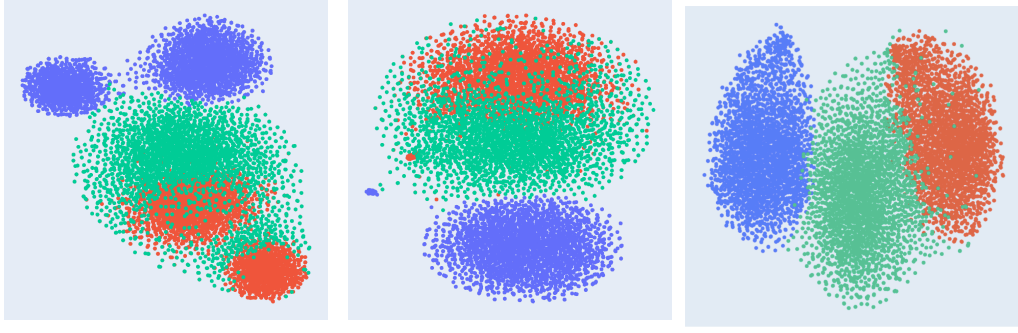
4.3.3 Multi-modal Humor Detection.

Further experiments are conducted on the UR-FUNNY dataset to verify the applicability of MInD. Since humor detection is sensitive to heterogeneous representations of different modalities, the best result achieved by MInD demonstrate the efficacy of our proposed multi-modal framework in learning distinct representations and capturing reliable information.

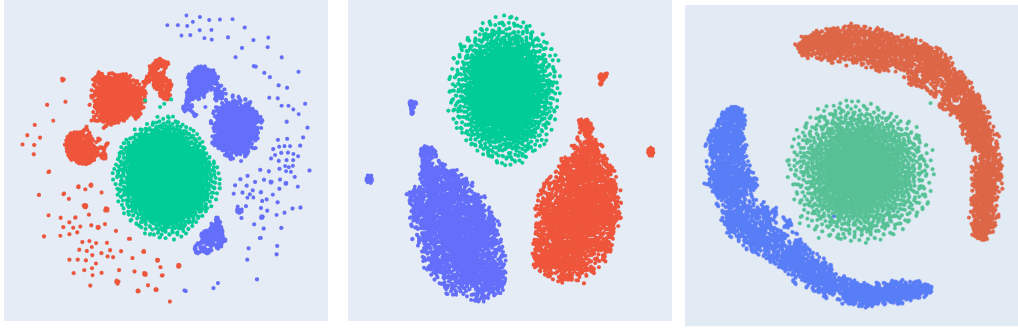
4.4 Ablation Studies

4.4.1 Role of Modality.

In Tab.2, we remove each modality separately to explore the performance of the bi-modal MInD, which performs consistently worse compared to the tri-modal MInD, suggesting that distinct modalities provides indispensable information. Specifically, we observe a significant drop in performance when we remove the text modality, yet similar drops are not observed in the other two cases. This shows the dominance of the text modality over the visual and audio modalities, probably due to the reason that the text modality contains manual transcriptions which could be inherently better, while on the contrary, the visual and audio modalities contain unfiltered raw signals with more noisy and redundant information.



(a) Visual, audio and text vectors before training, from left to right, respectively.



(b) Visual, audio and text vectors after training, from left to right, respectively.

Figure 2: We present the visualization results of noise vectors, as well as the modality-invariant and modality-specific components from distinct modalities, taking the testing set of UR-FUNNY as example. Blue: Invariant; Red: Specific; Green: Noise. MInD is able to depict different aspects of information.

4.4.2 Role of Disentanglement.

To empirically validate the effectiveness of the proposed disentanglement scheme, we carry out ablation studies on the modality-invariant components and the modality-specific components. As shown in Tab.2, muting any one of the components leads to a degraded performance, indicating that each set of components capture different aspects of the information and is hence essential and meaningful. In addition, we provide a non-disentangled version where the backbone features are directly utilized for fusion and prediction. This situation shows even worse results on MOSI and UR-FUNNY, which further demonstrates the effectiveness of our approach.

4.4.3 Role of Constraint.

As shown in Tab.2, all the constraints show non-trivial contribution to the performance of MInD. When there is no \mathcal{L}_{Info} , information extracted from the high-level features may be insufficient due to the adoption of simple shared and private encoders. This in turn demonstrates that with the help of well designed constraints, neural network models can be simple yet effective. When we remove \mathcal{L}_{Cons} or \mathcal{L}_{Diff} , model fails to capture the shared information or specific information of distinct modalities. In our model, \mathcal{L}_{Recon} and \mathcal{L}_{CyR} ensure the completeness and refinement of learned information, respectively. Removing them also brings worse performance. The removal of \mathcal{L}_{NP} leads to a slight degradation of performance on MOSEI and UR-FUNNY, and it is worth noting that the result on UR-FUNNY in this case still surpasses the baselines in Tab.2. Finally, we present the results trained only with \mathcal{L}_{Task} . The largest performance drop on most of the metrics demonstrates the necessity of all the constraints in our model.

4.5 Visualization

We visualize the noise vectors N_m , which are generated from Gaussian noise and subsequently aligned within the feature subspace by private encoders, along with the feature distributions of modality-invariant components S_m and modality-specific components P_m from individual modalities before and after training through T-SNE [48], using data from the testing set of UR-FUNNY.

As shown below, before training, there is no clear boundary between the modality-specific components and the synthetic noise. After training, the representations of the modality-specific components and the synthetic noise become more separated in the feature subspace, which helps a better exploitation of useful information. This illustrates the potential of MInD in isolating the meaningless information, thus facilitating better representations.

4.6 Experiment On Multi-modal Intent Recognition

In order to investigate the generality of our proposed framework on other affective computing tasks, we carry out further experiment on MIntRec [49] dataset for multi-modal intent recognition.

MIntRec includes 2,224 high-quality samples, divided into 1,334 for training, 445 for validation, and 445 for testing. This dataset is designed to categorize intents into two levels: coarse-grained and fine-grained. The coarse-grained level features binary intent labels, differentiating between expressing emotions or attitudes and pursuing goals. The fine-grained level provides a more detailed classification, with 20 intent labels: 11 related to expressing emotions or attitudes and 9 focused on goal achievement.

We compare MInD’s performance on the more difficult fine-grained level with the state-of-the-art multi-modal intent recognition methods, including MulT [14], MISA [8], MAG-BERT [50], SPECTRA [51] and CAGC [52]. The results are directly taken from their corresponding paper. As shown below, our model has achieved SOTA performance.

Methods	Acc-20	F1	Pre.	Rec.
MulT	72.52	69.25	70.25	69.24
MISA	72.29	69.32	70.85	69.24
MAG-BERT	72.65	68.64	69.08	69.28
SPECTRA	73.48	-	-	-
CAGC	73.39	70.09	71.21	70.39
MInD(Ours)	73.71	70.12	72.34	69.66

Table 3: Performance on MIntRec Dataset. Our results are highlighted in bold.

5 CONCLUSION

In this paper, we propose the Multi-modal Information Disentanglement (MInD) method to overcome the challenges caused by the inherent heterogeneity of distinct modalities through the decomposition of multi-modal inputs into modality-invariant and modality-specific components. We obtain the refined representations via the well-designed constraints and improve the quality of disentanglement with the help of explicitly training the generated noise in an adversarial manner, which provides a new insight to pay attention to the meaningless information during the learning of different representation subspace. Experimental results demonstrate the superiority of our method. In the future, we plan to broaden the application spectrum of our method, deploying it across a diverse array of multi-modal scenarios.

References

- [1] Soujanya Poria, Devamanyu Hazarika, Navonil Majumder, and Rada Mihalcea. Beneath the tip of the iceberg: Current challenges and new directions in sentiment analysis research. *IEEE Transactions on Affective Computing*, 2020.
- [2] Amir Zadeh, Minghai Chen, Soujanya Poria, Erik Cambria, and Louis-Philippe Morency. Tensor fusion network for multimodal sentiment analysis. *arXiv preprint arXiv:1707.07250*, 2017.
- [3] Yu Huang, Chenzhuang Du, Zihui Xue, Xuanyao Chen, Hang Zhao, and Longbo Huang. What makes multi-modal learning better than single (provably). *Advances in Neural Information Processing Systems*, 34:10944–10956, 2021.
- [4] Victor Weixin Liang, Yuhui Zhang, Yongchan Kwon, Serena Yeung, and James Y Zou. Mind the gap: Understanding the modality gap in multi-modal contrastive representation learning. *Advances in Neural Information Processing Systems*, 35:17612–17625, 2022.
- [5] Hai Pham, Paul Pu Liang, Thomas Manzini, Louis-Philippe Morency, and Barnabás Póczos. Found in translation: Learning robust joint representations by cyclic translations between modalities. In *Proceedings of the AAAI Conference on Artificial Intelligence*, volume 33, pages 6892–6899, 2019.

- [6] Sijie Mai, Haifeng Hu, and Songlong Xing. Modality to modality translation: An adversarial representation learning and graph fusion network for multimodal fusion. In *Proceedings of the AAAI Conference on Artificial Intelligence*, volume 34, pages 164–172, 2020.
- [7] Konstantinos Bousmalis, George Trigeorgis, Nathan Silberman, Dilip Krishnan, and Dumitru Erhan. Domain separation networks. *Advances in neural information processing systems*, 29, 2016.
- [8] Devamanyu Hazarika, Roger Zimmermann, and Soujanya Poria. Misa: Modality-invariant and-specific representations for multimodal sentiment analysis. In *Proceedings of the 28th ACM international conference on multimedia*, pages 1122–1131, 2020.
- [9] Dingkan Yang, Shuai Huang, Haopeng Kuang, Yangtao Du, and Lihua Zhang. Disentangled representation learning for multimodal emotion recognition. In *Proceedings of the 30th ACM International Conference on Multimedia*, pages 1642–1651, 2022.
- [10] Ashish Vaswani, Noam Shazeer, Niki Parmar, Jakob Uszkoreit, Llion Jones, Aidan N Gomez, Łukasz Kaiser, and Illia Polosukhin. Attention is all you need. *Advances in neural information processing systems*, 30, 2017.
- [11] Aman Shenoy and Ashish Sardana. Multilogue-net: A context aware rnn for multi-modal emotion detection and sentiment analysis in conversation. *arXiv preprint arXiv:2002.08267*, 2020.
- [12] Md Shad Akhtar, Dushyant Singh Chauhan, Deepanway Ghosal, Soujanya Poria, Asif Ekbal, and Pushpak Bhattacharyya. Multi-task learning for multi-modal emotion recognition and sentiment analysis. *arXiv preprint arXiv:1905.05812*, 2019.
- [13] Jiasen Lu, Jianwei Yang, Dhruv Batra, and Devi Parikh. Hierarchical question-image co-attention for visual question answering. *Advances in neural information processing systems*, 29, 2016.
- [14] Yao-Hung Hubert Tsai, Shaojie Bai, Paul Pu Liang, J Zico Kolter, Louis-Philippe Morency, and Ruslan Salakhutdinov. Multimodal transformer for unaligned multimodal language sequences. In *Proceedings of the conference. Association for Computational Linguistics. Meeting*, volume 2019, page 6558. NIH Public Access, 2019.
- [15] Jean-Benoit Delbrouck, Noé Tits, Mathilde Brousmiche, and Stéphane Dupont. A transformer-based joint-encoding for emotion recognition and sentiment analysis. *arXiv preprint arXiv:2006.15955*, 2020.
- [16] Hyunjik Kim and Andriy Mnih. Disentangling by factorising. In *International Conference on Machine Learning*, pages 2649–2658. PMLR, 2018.
- [17] Mathieu Salzmann, Carl Henrik Ek, Raquel Urtasun, and Trevor Darrell. Factorized orthogonal latent spaces. In *Proceedings of the thirteenth international conference on artificial intelligence and statistics*, pages 701–708. JMLR Workshop and Conference Proceedings, 2010.
- [18] Weikuo Guo, Huaibo Huang, Xiangwei Kong, and Ran He. Learning disentangled representation for cross-modal retrieval with deep mutual information estimation. In *Proceedings of the 27th ACM International Conference on Multimedia*, pages 1712–1720, 2019.
- [19] Wenyi Tang, Bei Hui, Ling Tian, Guangchun Luo, Zaobo He, and Zhipeng Cai. Learning disentangled user representation with multi-view information fusion on social networks. *Information Fusion*, 74:77–86, 2021.
- [20] Jacob Devlin, Ming-Wei Chang, Kenton Lee, and Kristina Toutanova. Bert: Pre-training of deep bidirectional transformers for language understanding. *arXiv preprint arXiv:1810.04805*, 2018.
- [21] Yi Zhang, Mingyuan Chen, Jundong Shen, and Chongjun Wang. Tailor versatile multi-modal learning for multi-label emotion recognition. In *Proceedings of the AAAI Conference on Artificial Intelligence*, volume 36, pages 9100–9108, 2022.
- [22] Dan Hendrycks and Kevin Gimpel. Gaussian error linear units (gelus). *arXiv preprint arXiv:1606.08415*, 2016.
- [23] R Devon Hjelm, Alex Fedorov, Samuel Lavoie-Marchildon, Karan Grewal, Phil Bachman, Adam Trischler, and Yoshua Bengio. Learning deep representations by mutual information estimation and maximization. *arXiv preprint arXiv:1808.06670*, 2018.
- [24] Jure Zbontar, Li Jing, Ishan Misra, Yann LeCun, and Stéphane Deny. Barlow twins: Self-supervised learning via redundancy reduction. In *International Conference on Machine Learning*, pages 12310–12320. PMLR, 2021.
- [25] Yao-Hung Hubert Tsai, Shaojie Bai, Louis-Philippe Morency, and Ruslan Salakhutdinov. A note on connecting barlow twins with negative-sample-free contrastive learning. *arXiv preprint arXiv:2104.13712*, 2021.
- [26] Le Song, Alex Smola, Arthur Gretton, Karsten M Borgwardt, and Justin Bedo. Supervised feature selection via dependence estimation. In *Proceedings of the 24th international conference on Machine learning*, pages 823–830, 2007.

- [27] Yaroslav Ganin, Evgeniya Ustinova, Hana Ajakan, Pascal Germain, Hugo Larochelle, François Laviolette, Mario March, and Victor Lempitsky. Domain-adversarial training of neural networks. *Journal of machine learning research*, 17(59):1–35, 2016.
- [28] Amir Zadeh, Rowan Zellers, Eli Pincus, and Louis-Philippe Morency. Multimodal sentiment intensity analysis in videos: Facial gestures and verbal messages. *IEEE Intelligent Systems*, 31(6):82–88, 2016.
- [29] AmirAli Bagher Zadeh, Paul Pu Liang, Soujanya Poria, Erik Cambria, and Louis-Philippe Morency. Multimodal language analysis in the wild: Cmu-mosei dataset and interpretable dynamic fusion graph. In *Proceedings of the 56th Annual Meeting of the Association for Computational Linguistics (Volume 1: Long Papers)*, pages 2236–2246, 2018.
- [30] Md Kamrul Hasan, Wasifur Rahman, Amir Zadeh, Jianyuan Zhong, Md Iftekhhar Tanveer, Louis-Philippe Morency, et al. Ur-funny: A multimodal language dataset for understanding humor. *arXiv preprint arXiv:1904.06618*, 2019.
- [31] Jeffrey Pennington, Richard Socher, and Christopher D Manning. Glove: Global vectors for word representation. In *Proceedings of the 2014 conference on empirical methods in natural language processing (EMNLP)*, pages 1532–1543, 2014.
- [32] Gilles Degottex, John Kane, Thomas Drugman, Tuomo Raitio, and Stefan Scherer. Covarep—a collaborative voice analysis repository for speech technologies. In *2014 IEEE international conference on acoustics, speech and signal processing (icassp)*, pages 960–964. IEEE, 2014.
- [33] Tadas Baltrušaitis, Peter Robinson, and Louis-Philippe Morency. Openface: an open source facial behavior analysis toolkit. In *2016 IEEE winter conference on applications of computer vision (WACV)*, pages 1–10. IEEE, 2016.
- [34] Zhun Liu, Ying Shen, Varun Bharadhwaj Lakshminarasimhan, Paul Pu Liang, Amir Zadeh, and Louis-Philippe Morency. Efficient low-rank multimodal fusion with modality-specific factors. *arXiv preprint arXiv:1806.00064*, 2018.
- [35] Yao-Hung Hubert Tsai, Paul Pu Liang, Amir Zadeh, Louis-Philippe Morency, and Ruslan Salakhutdinov. Learning factorized multimodal representations. *arXiv preprint arXiv:1806.06176*, 2018.
- [36] Zhongkai Sun, Prathusha Sarma, William Sethares, and Yingyu Liang. Learning relationships between text, audio, and video via deep canonical correlation for multimodal language analysis. In *Proceedings of the AAAI Conference on Artificial Intelligence*, volume 34, pages 8992–8999, 2020.
- [37] Wenmeng Yu, Hua Xu, Ziqi Yuan, and Jiele Wu. Learning modality-specific representations with self-supervised multi-task learning for multimodal sentiment analysis. In *Proceedings of the AAAI conference on artificial intelligence*, volume 35, pages 10790–10797, 2021.
- [38] Sijie Mai, Ying Zeng, Shuangjia Zheng, and Haifeng Hu. Hybrid contrastive learning of tri-modal representation for multimodal sentiment analysis. *IEEE Transactions on Affective Computing*, 2022.
- [39] Wei Han, Hui Chen, Alexander Gelbukh, Amir Zadeh, Louis-philippe Morency, and Soujanya Poria. Bi-bimodal modality fusion for correlation-controlled multimodal sentiment analysis. In *Proceedings of the 2021 International Conference on Multimodal Interaction*, pages 6–15, 2021.
- [40] Hao Sun, Hongyi Wang, Jiaqing Liu, Yen-Wei Chen, and Lanfen Lin. Cubemlp: An mlp-based model for multimodal sentiment analysis and depression estimation. In *Proceedings of the 30th ACM International Conference on Multimedia*, pages 3722–3729, 2022.
- [41] Peipei Liu, Xin Zheng, Hong Li, Jie Liu, Yimo Ren, Hongsong Zhu, and Limin Sun. Improving the modality representation with multi-view contrastive learning for multimodal sentiment analysis. In *ICASSP 2023-2023 IEEE International Conference on Acoustics, Speech and Signal Processing (ICASSP)*, pages 1–5. IEEE, 2023.
- [42] Kyeonghun Kim and Sanghyun Park. Aobert: All-modalities-in-one bert for multimodal sentiment analysis. *Information Fusion*, 92:37–45, 2023.
- [43] Yewon Hwang and Jong-Hwan Kim. Self-supervised unimodal label generation strategy using recalibrated modality representations for multimodal sentiment analysis. In *Findings of the Association for Computational Linguistics: EACL 2023*, pages 35–46, 2023.
- [44] Jiuding Yang, Yakun Yu, Di Niu, Weidong Guo, and Yu Xu. Confede: Contrastive feature decomposition for multimodal sentiment analysis. In *Proceedings of the 61st Annual Meeting of the Association for Computational Linguistics (Volume 1: Long Papers)*, pages 7617–7630, 2023.
- [45] Daoming Zong, Chaoyue Ding, Baoxiang Li, Jiakui Li, Ken Zheng, and Qunyan Zhou. Acformer: An aligned and compact transformer for multimodal sentiment analysis. In *Proceedings of the 31st ACM International Conference on Multimedia*, pages 833–842, 2023.

- [46] Jingming Hou, Nazlia Omar, Sabrina Tiun, Saidah Saad, and Qian He. Tchfn: Multimodal sentiment analysis based on text-centric hierarchical fusion network. *Knowledge-Based Systems*, 300:112220, 2024.
- [47] Youjia Fu, Junsong Fu, Huixia Xue, and Zihao Xu. Self-hcl: Self-supervised multitask learning with hybrid contrastive learning strategy for multimodal sentiment analysis. *Electronics*, 13(14):2835, 2024.
- [48] Laurens Van der Maaten and Geoffrey Hinton. Visualizing data using t-sne. *Journal of machine learning research*, 9(11), 2008.
- [49] Hanlei Zhang, Hua Xu, Xin Wang, Qianrui Zhou, Shaojie Zhao, and Jiayan Teng. Mintrec: A new dataset for multimodal intent recognition. In *Proceedings of the 30th ACM International Conference on Multimedia*, pages 1688–1697, 2022.
- [50] Wasifur Rahman, Md Kamrul Hasan, Sangwu Lee, Amir Zadeh, Chengfeng Mao, Louis-Philippe Morency, and Ehsan Hoque. Integrating multimodal information in large pretrained transformers. In *Proceedings of the conference. Association for Computational Linguistics. Meeting*, volume 2020, page 2359. NIH Public Access, 2020.
- [51] Tianshu Yu, Haoyu Gao, Ting-En Lin, Min Yang, Yuchuan Wu, Wentao Ma, Chao Wang, Fei Huang, and Yongbin Li. Speech-text pre-training for spoken dialog understanding with explicit cross-modal alignment. In *Proceedings of the 61st Annual Meeting of the Association for Computational Linguistics (Volume 1: Long Papers)*, pages 7900–7913, 2023.
- [52] Kaili Sun, Zhiwen Xie, Mang Ye, and Huyin Zhang. Contextual augmented global contrast for multimodal intent recognition. In *Proceedings of the IEEE/CVF Conference on Computer Vision and Pattern Recognition*, pages 26963–26973, 2024.